



A Journal of the Gesellschaft Deutscher Chemiker

Angewandte Chemie

GDCh

International Edition

www.angewandte.org

Accepted Article

Title: Double Fence Porphyrins that are Compatible with Coll/III Electrolyte for High Efficiency Dye-Sensitized Solar Cells

Authors: Ching-Chin Chen, Jia-Sian Chen, Vinh Son Nguyen, Tzu-Chien Wei, and Chen-Yu Yeh

This manuscript has been accepted after peer review and appears as an Accepted Article online prior to editing, proofing, and formal publication of the final Version of Record (VoR). This work is currently citable by using the Digital Object Identifier (DOI) given below. The VoR will be published online in Early View as soon as possible and may be different to this Accepted Article as a result of editing. Readers should obtain the VoR from the journal website shown below when it is published to ensure accuracy of information. The authors are responsible for the content of this Accepted Article.

To be cited as: *Angew. Chem. Int. Ed.* 10.1002/anie.202013964

Link to VoR: <https://doi.org/10.1002/anie.202013964>

RESEARCH ARTICLE

Double Fence Porphyrins that are Compatible with Co^{II/III} Electrolyte for High Efficiency Dye-Sensitized Solar Cells

Ching-Chin Chen,^{[a][b]} Jia-Sian Chen,^[a] Vinh Son Nguyen,^[b] Tzu-Chien Wei,^{*[b]} Chen-Yu Yeh^{*[a]}

- [a] Dr. C.-C. Chen, J.-S. Chen, Prof. C.-Y. Yeh
Department of Chemistry, *i*-Center for Advanced Science and Technology (*i*-CAST), Innovation and Development Center of Sustainable Agriculture (IDCSA)
National Chung Hsing University
No. 145, Xingda Rd., South Dist., Taichung City 402, Taiwan
E-mail: cyeh@dragon.nchu.edu.tw
- [b] Dr. C.-C. Chen, V. S. Nguyen, Prof. T.-Z. Wei
Department of Chemical Engineering
National Tsing-Hua University
No. 101, Sec. 2, Guangfu Rd., East Dist., Hsinchu City 300, Taiwan
E-mail: tcwei@mx.nthu.tw

Supporting information for this article is given via a link at the end of the document.

Abstract: A series of new double fence porphyrin dyes **bJS1–bJS3** with eight long alkoxy chains attached to the four β -phenyl groups have been designed and synthesized. The single fence *meso*-substituted counterparts **mJS1–mJS3** were also prepared as reference dyes. Dyes **bJS1–bJS3** and **mJS1–mJS3** exhibit power conversion efficiency of 8.03%–10.69% and 2.33%–6.69%, respectively. The remarkable cell performance of double fence porphyrin sensitizers can be attributed to reduced dye aggregation and decreased charge recombination rate based on photovoltaic studies. It should be noted that porphyrins **bJS2** and **bJS3** exhibit better efficiency than the benchmark **YD2-o-C8** (9.83% in this work), demonstrating that the double fence structure is a promising design strategy for efficient porphyrin sensitizers in high performance DSSCs.

Introduction

The use of renewable energy resources has been an important issue for sustainable development of human society. Among all sustainable energy resources, solar power is the most abundant one that can provide more than enough energy for global energy demand. Thus, conversion of solar energy to electricity or chemical energy has attracted much attention over the past decades. Currently, crystalline silicon solar cells which show high power conversion efficiency (PCE) up to 25% hold 90% of global market share of commercial solar cells.^[1] However, the material- and energy-cost process as well as long energy payback time for manufacturing of silicon-based solar cells have prompted researchers to develop new types of photovoltaic technology.^[2] Dye-sensitized solar cells (DSSCs) which belong to a new generation of photovoltaic techniques were invented by Grätzel in 1991.^[3] Compared to silicon-based solar cells, DSSCs have several advantages such as feasible fabrication process, low production cost, environmental friendliness, colorfulness, high efficiency under dim light and high-flexibility.^[4] The device of a DSSC consists of a working electrode, a sensitizer, electrolytes, and a counter electrode. These components have been

extensively studied to enhance photovoltaic performance of DSSCs in the past decades.^[5] As sunlight absorber in DSSCs, the sensitizer is a crucial component, of which its properties can be tuned by molecular modification to achieve high efficiency of the devices. In general, there are four types of sensitizers including ruthenium-based complexes, metal-free dyes, porphyrins, and natural pigments.^[6] To date, the benchmark PCE of DSSCs was reported to be > 12% using porphyrin-based photosensitizers such as **SM315**, **SGT-021**, and **GY50** under illumination of standard AM 1.5G simulated sunlight (1000 W/m²).^[5d,7]

Porphyrins and their derivatives have intense Soret band (400 ~ 500 nm) and moderate Q-band (500 ~ 600 nm) in the visible region^[8] and the absorption broadness and strength of porphyrins can be readily tailored by molecular engineering to enhance their light-harvesting ability. The superior absorption properties of porphyrins make them promising sensitizers for DSSCs. However, porphyrin-based sensitizers had been suffering from low device performance (PCE < 7.1%) until **YD**-series of porphyrins were reported.^[9] With the particular donor- π -acceptor (D- π -A) molecular structure to enhance light-harvesting and electron injection efficiency, **YD2** reached a PCE as high as 11%, which is comparable with the most efficient ruthenium-based dyes such as **N719** and black dye for DSSCs.^[10] Later, further modification of dye **YD2** was performed by introduction of long alkoxy groups to the *ortho*-positions of *meso*-phenyls of the porphyrin ring to afford dye **YD2-o-C8** (Figure 1), which is compatible with Co^{II/III}tris(2,2'-bipyridyl) redox shuttle, leading to a remarkable PCE of 11.9% for the device.^[5i] Sterically hindered long alkoxy chains not only reduce aggregation of dye molecules but also suppress charge recombination between TiO₂ and electrolyte, leading to enhancement of short-circuit photocurrent (J_{sc}) and open-circuit voltage (V_{oc}), thus improved PCE of the device. Meanwhile, to improve the cell performance, various strategies for devices of porphyrins other than the D- π -A structural design have been reported, such as co-sensitization,^[5i,11] broadening absorption spectra,^[5e,12] modification of anchoring groups,^[13] donor and acceptor unit,^[7a,14] and co-adsorption.^[15] All these molecular design strategies showed more or less improvement on

RESEARCH ARTICLE

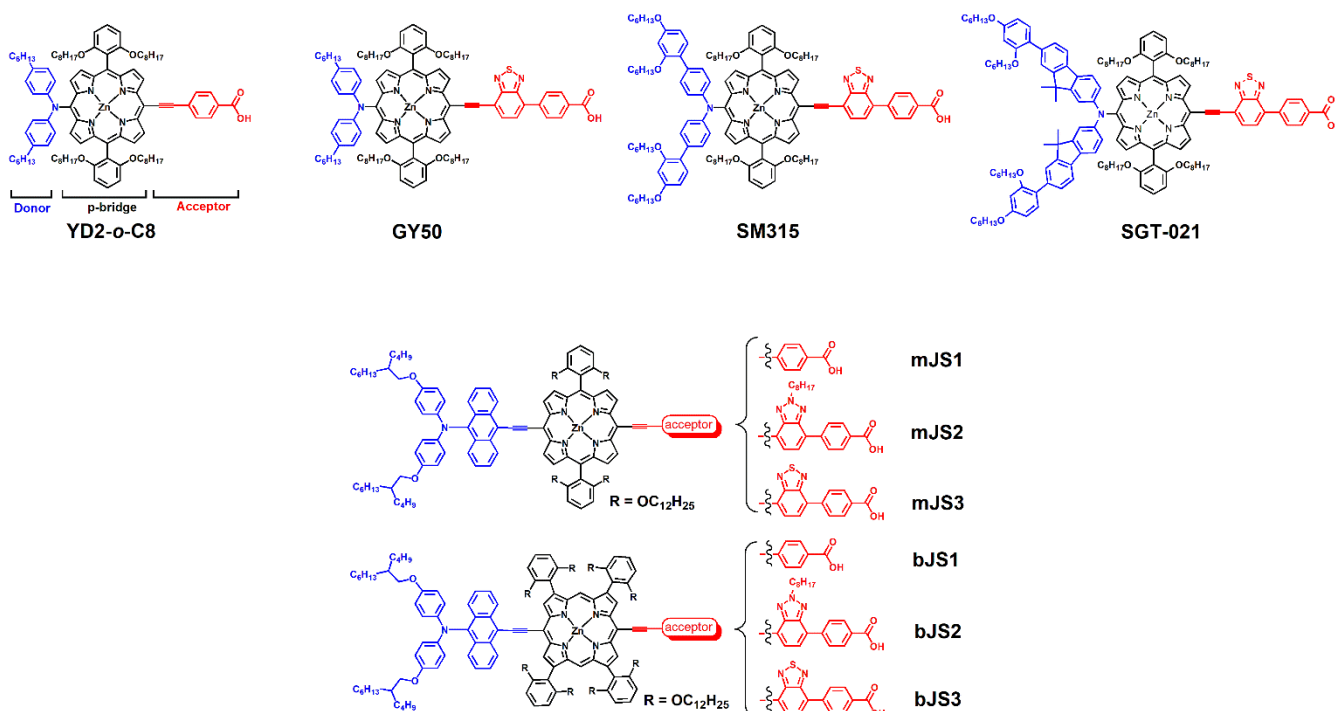


Figure 1. Structure of efficient porphyrin-based sensitizers.

PCE of DSSCs. However, introduction of long-chain alkoxy groups and D- π -A structure is the essential requirements of an efficient porphyrin dye as cobalt electrolytes are used. Compared to dye **GY50**, the slightly better performance of **SM315** indicates that introduction of more alkoxy groups to a bulky donor moiety is a useful strategy to further improve PCE and similar results were also reported for **XW**- and **SGT**-series of porphyrins.^[14a,16] Based on the molecular structures, all these efficient sensitizers share a common porphyrin core structure with the porphyrin ring being wrapped by four long alkoxy chains, which would form a hydrophobic environment on the surface of TiO₂ to impede the approach of charged electrolytes. In such a case, the *meso*-phenyls with long alkoxy chains can be considered as an effective “fence” to suppress dye aggregation and charge recombination.

To further attenuate charge recombination and molecular aggregation, we designed novel “double fence” porphyrin sensitizers **bJS1**, **bJS2** and **bJS3** with four β -phenyl rings substituted with long alkoxy groups at the *ortho*-positions as shown in Figure 1, and the architecture of single and double fence porphyrin dyes are depicted in Figure 2. In addition, anthracene-containing triaryl amino group was employed as a donor with dual functions, electron-donating and absorption-broadening.^[17] Incorporation of benzotriazole (BTA) and benzothiadiazole (BTD) unit in acceptor moiety for **bJS2** and **bJS3**, respectively, causes further red-shift of the absorption, thus enhancing light-harvesting

capability. Introduction of BTD and BTA unit in their single fence analogues **mJS** dyes were also synthesized as references to better understand the effect of β -substituted alkoxy-phenyl groups. Based on the photovoltaic studies, double fence porphyrins exhibited much higher J_{SC} and V_{oc} than single fence porphyrins using Co^{III}/tris(2,2'-bipyridyl) as redox electrolyte. Thus, **bJS2** and **bJS3** achieved remarkable PCE of 10.69% and 10.42% while **mJS2** and **mJS3** only exhibited PCE of 3.48% and 2.33% under illumination of AM 1.5G simulated sunlight. It is noteworthy that porphyrins **bJS2** and **bJS3** show higher efficiency as compared to benchmark **YD2-o-C8** ($\eta = 9.83\%$) under similar conditions.

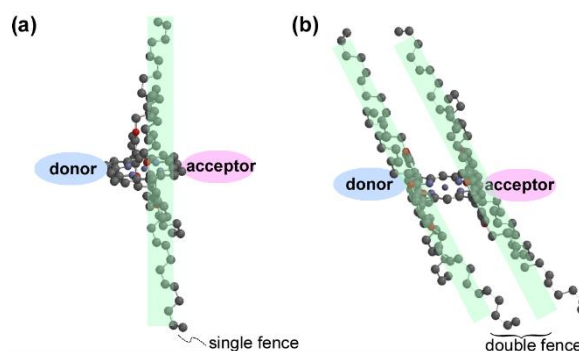
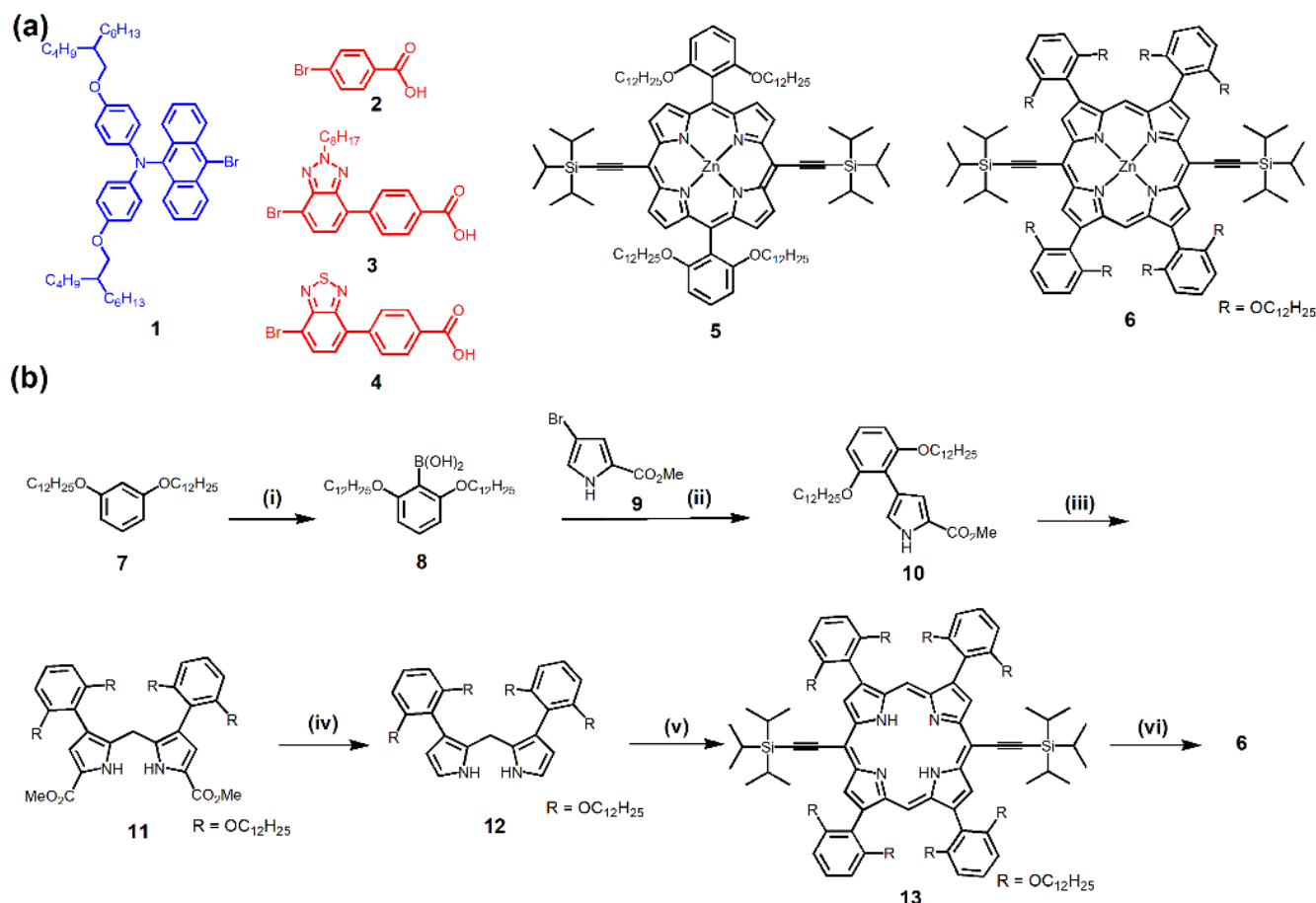


Figure 2. Architecture of (a) single fence and (b) double fence porphyrins.

RESEARCH ARTICLE



Scheme 1. (a) Chemical structures of donor moiety, acceptor moiety, and porphyrin precursors. (b) Synthetic route of novel β -substituted porphyrin. (i) *n*-BuLi, trimethylborate, THF. (ii) Pd(PPh₃)₄, 2 M Na₂CO_{3(aq)}, 1,4-dioxane. (iii) Dimethoxymethane, BF₃·Et₂O, CH₂Cl₂. (iv) KOH, (CH₂O)₂. (v) 3-(triisopropylsilyl)-1-propynal, BF₃·Et₂O, CH₂Cl₂. (vi) Zn(OAc)₂·2H₂O, CH₂Cl₂/ MeOH.

Results and Discussion

Most of efficient porphyrins are based on a 5,10,15,20-*meso*-substituted structure because structural modification at the *meso*-positions of porphyrins is more accessible than at the β -positions. As mentioned, efficient porphyrin sensitizers have a commonly used core, i.e., 5,15-bis(2,6-dialkoxyphenyl)porphyrin, and the porphyrin ring is wrapped by four long alkoxy chains. To improve the light-harvesting capability of dyes, and thus the cell performance of devices, the most widely used strategy is to extend the π -conjugation by insertion of acetylene and/or a variety of aromatic units to the D- π -A architecture. However, such a strategy induces more severe molecular aggregation so that excess co-adsorbent such as CDCA has to be employed for device fabrication in order to enhance the cell performance.^[17a] Obviously, introduction of more long alkoxy chains to wrap the porphyrin ring would outperform previously used system with only four alkoxy chains. Therefore, in this work judiciously tailored double fence porphyrins were designed and synthesized with aims of reducing dye aggregation and impeding charge recombination. The synthetic route of novel β -substituted zinc porphyrin **6** is shown in Scheme 1 and the synthetic procedures are detailed in Supporting Information. Anthracene-containing triphenyl amine donor moiety **1**, benzothiazole-containing acceptor moiety **3**, benzothiadiazole-containing acceptor moiety **4**,

and *meso*-substituted porphyrin precursor **5** were prepared as previously reported.^[4c,18] The key intermediate pyrrole **10** was synthesized via Suzuki coupling using bromopyrrole **9** and boronic acid **8** which were prepared as reported procedures.^[18a,19] The reaction of pyrrole **10** with dimethoxymethane afforded dipyrromethane **11**, which was then decarboxylated under alkaline conditions to give **12**. Condensation of **12** with 3-(triisopropylsilyl)-1-propynal^[20] followed by oxidation and metalation afforded β -substituted zinc porphyrin **6**. The **mJS**-series and **bJS**-series dyes were synthesized via Sonogashira coupling using the corresponding porphyrin precursors, which were obtained by desilylation of **5** and **6** with tetra-*n*-butylammonium fluoride (TBAF), respectively, with appropriate donor/acceptor moieties.

The UV-vis spectra of **mJS** and **bJS** porphyrin sensitizers in THF are displayed in Figure 3, and the absorption and emission data are collected in Table 1. Energy levels of porphyrin frontier orbitals can be perturbed by *meso*- and β -substituents, thus the excitation energy of porphyrin would be modulated according to the Gouterman's four-orbital model.^[8] These new porphyrin dyes exhibit more red-shifted and broadened absorptions with respect to simple porphyrins such as 5,10,15,20-tetraarylporphyrin and the Soret band is red-shifted (by 10-30 nm) and Q-bands are slightly blue-shifted (by 6-7 nm) for the double fence **bJS** porphyrins as compared to those of single fence **mJS** dyes. Similar to **LWP14** reported by Lin and coworkers,^[17a] these

RESEARCH ARTICLE

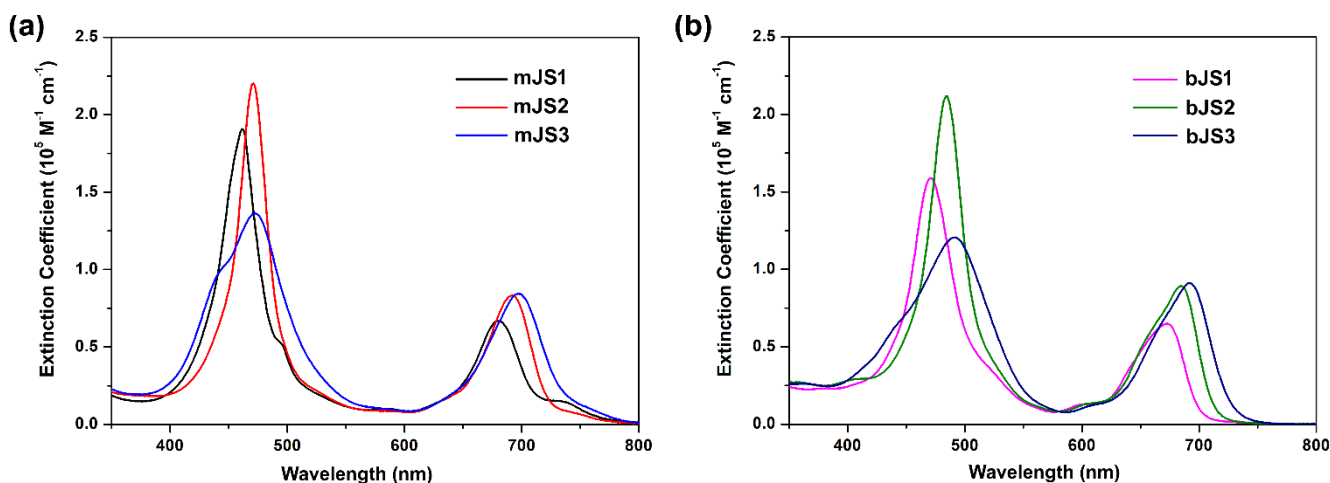


Figure 3. Absorption spectra of (a) **mJS** and (b) **bJS** dyes.

anthracene-containing porphyrin dyes show a strong and broad Soret band in a range of 462 to 492 nm and a moderate Q-band in a range of 673 to 698 nm, in which their Soret and Q bands are both more red-shifted with respect to anthracene-free high efficiency porphyrins **SM315** and **GY50** owing to more extended π -system.^[5d,5e] Among these dyes, **bJS2** and **mJS2** have the highest maximum molar absorption coefficient compared to their corresponding series of porphyrins, respectively. Insertion of bridge 2,1,3-benzothiadiazole (BTD) or 1,2,3-benzotriazole (BTA) between benzoic acid and acetylene moieties causes red-shift of both Soret and Q band, thus increasing the light harvesting capability. Such a phenomenon has also been observed for **GY50** and **SM315**.

To evaluate energy levels of frontier orbitals, cyclic voltammetry (CV) was employed to investigate the electrochemical properties of **mJS**- and **bJS**- series of dyes using THF and 0.1 M tetrabutylammonium hexafluorophosphate (TBAPF₆) as solvent and supporting electrolyte, respectively. The results are presented in Figure 4 and Table 1. The energy levels of highest occupied molecular orbital (E_{HOMO}) were determined with redox potential ($E_{1/2(\text{ox})}$) of the first oxidation for each sensitizer using ferrocene/ferrocenium (Fc/Fc^+ , $E_{1/2} = 0.63$ V vs. normal hydrogen

electrode, NHE) as an internal standard. Energy levels of the first excited states of sensitizers were estimated from E_{HOMO} and optical bandgap (E_{0-0}), which was obtained from the cross section of absorption and emission spectra, by the equation $E_{\text{S}_1} = E_{\text{HOMO}} - E_{0-0}$. The optical band gap of dye **mJS2**, **mJS3**, **bJS2**, and **bJS3** are in a range of 1.74 to 1.79 eV, which is smaller than that of **GY50** (1.81 eV) ascribed to the extended π -conjugation by incorporating acetylene and anthracene unit to the donor moiety, whereas dye **mJS1** (1.81 V vs. NHE) and **bJS1** (1.83 V vs. NHE) built without electron-deficient BTD or BTA unit in acceptor moiety have higher optical band gap. In comparison with **mJS** dyes, the HOMO and S_1 (the first excited state) of **bJS** dyes are destabilized by only 0.03 eV and 0.05 eV, respectively, indicating the numbers and positions of phenyl substitution only slightly disturb the electronic structure of porphyrins because the dihedral angles between porphyrin and phenyl rings are in the range 65-90 degrees. The HOMO levels of **mJS**- and **bJS**- series (0.91 to 0.82 V vs. NHE) are lower than those of **GY50** and **YD2-o-C8** (0.79 and 0.82 V vs. NHE), providing enough driving force for dye regeneration. Furthermore, all the first excited levels are considerably higher than the conduction band of TiO₂. Thus, efficient electron injection can be expected.

Table 1. Optical and Electrochemical Properties of Sensitizers **mJS** and **bJS**.

dye	Absorption λ_{max} , [ϵ] ^[a] (nm), [(10 ⁵ M ⁻¹ cm ⁻¹)]	Emission λ_{max} ^[a] (nm)	E_{HOMO} ^[b] (V vs. NHE)	E_{S_1} ^[c] (V vs. NHE)	E_{0-0} ^[d] (eV)
mJS1	462[1.91], 679[0.67]	700	0.91	-0.90	1.81
mJS2	471[2.20], 692[0.84]	709	0.85	-0.92	1.77
mJS3	472[1.36], 697[0.85]	734	0.86	-0.88	1.74
bJS1	471[1.59], 673[0.65]	685	0.87	-0.96	1.83
bJS2	484[2.12], 685[0.89]	699	0.82	-0.97	1.79
bJS3	492[1.21], 691[0.91]	723	0.83	-0.93	1.76

[a] Wavelength maxima for absorption (including Soret and Q- band) and emission are record in THF at 25 °C. [b] Determined by cyclic voltammetry (CV) in THF containing 0.1 M tetrabutylammonium hexafluorophosphate (TBAPF₆) as electrolyte and was calibrated with ferrocene/ferrocenium (Fc/Fc^+) as internal reference at 25 °C. [c] Energy level of first excited state (S_1) was calculated by following equation: $E_{\text{S}_1} = E_{\text{HOMO}} - E_{0-0}$. [d] Determined from the intersection of normalized absorption and emission spectra in THF.

RESEARCH ARTICLE

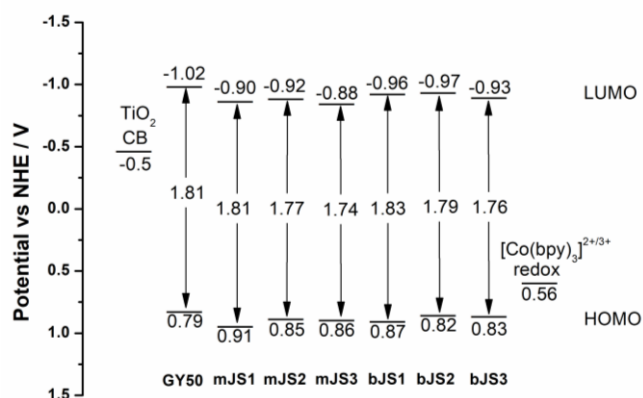


Figure 4. Schematic energy level diagram of **mJS1**, **mJS2**, **mJS3**, **bJS1**, **bJS2**, and **bJS3** based on their electrochemical and optical data.

To gain further insight into the ground state geometry and electron density distribution of the porphyrins, density functional theory (DFT) calculations were performed on model porphyrins and the results are displayed in Figure S32. Upon geometry optimization, the porphyrin macrocycle remains planar for both **mJS** and **bJS** series of porphyrins because the dialkoxylphenyl groups at *meso*- or β -positions are far away from coplanar to the porphyrin ring (dihedral angles between phenyl ring and porphyrin core: -90° for **mJS** and 65° – 70° for **bJS**) so that no steric interaction between phenyl groups was observed. As expected, the BTD and BTA unit adopt nearly coplanar conformation with the porphyrin core, providing effective π -conjugation of the donor- π -acceptor backbone. The dihedral angle between anthracene and porphyrin plane are around 29° in all **mJS** and **bJS** dyes ascribed to the steric interaction between 1,2-H atoms of anthracene and the two closest β -H atoms of porphyrin ring, which is similar to that in Mg-TIPSTEP-anthryl (ca. 41°), a magnesium porphyrin containing ethynyl-bridged anthracene unit reported by Marsuo *et al.*^[21] The optimized structures are consistent with the red-shifted and broadened absorption spectra due to effective electronic interaction among donor, porphyrin core, and acceptor in all these new dyes via acetylene bridges. The calculated HOMO–LUMO gaps obtained from DFT calculations are 2.27 eV for **YD2-o-C8**, 1.92 eV for **mJS1**, 1.90 eV for **mJS2**, 1.84 eV for **mJS3**, 1.96 eV for **bJS1**, 1.96 eV for **bJS2**, and 1.88 eV for **bJS3**, respectively, and the trend of calculated HOMO–LUMO gaps are consistent with experimental HOMO–LUMO gaps obtained from optical data. The orbital distribution of HOMO is mainly populated on the electron-donating group and slightly on the porphyrin *meso*-carbons and nitrogens for all these new porphyrins. On the other hand, the LUMO are mainly localized on porphyrin ring and acceptor moiety in all porphyrins, in which BTD unit has more contribution than BTA unit. Therefore, BTD-containing **mJS3** and **bJS3** have lower LUMO energy level than BTA-incorporated **mJS2** and **bJS2**. It is worthy to note that the LUMO are also populated on the acetylene bridge in **mJS1** and **bJS1** series, which leads to lower LUMO energy level than **YD2-o-C8**, implying that the acetylene bridge not only destabilizes HOMO but also stabilizes LUMO of porphyrin sensitizers. As a result, a decreasing HOMO–LUMO gap is observed for these new porphyrins. Further, the excitation behavior of these new

porphyrin dyes was theoretically investigated via time-dependent DFT (TDDFT) calculation at the same level, the result was collected in Table S1 to Table S6. The TDDFT calculations shows that the Soret and Q bands of all these porphyrin dyes are dominated by HOMO-2 to LUMO+1 and HOMO to LUMO transitions, respectively, regardless the type and position of peripheral substituents. Four selected frontier orbitals including HOMO-2, HOMO, LUMO, and LUMO+1 of **mJS1** and **bJS1** are shown in Figure S33. The electron-donating β -phenyl substituents would raise the energy level of HOMO-2 and LUMO, which have significant electron density on the β -carbons, for **bJS** dyes. Similarly, the HOMO is raised in **mJS** dyes owing to electron-donating *meso*-phenyl groups as shown in Figure S33. Therefore, **bJS** dyes would have red-shifted Soret band and blue-shifted Q bands, consistent with what have been observed in UV-vis spectra.

It is well known that porphyrin sensitizers wrapped by long alkoxy groups exhibit better device performance with $[\text{Co}(\text{bpy})_3]^{3+/2+}$ than I^-/I_3^- redox couple because of significantly suppressed charge recombination process between TiO_2 electron and $[\text{Co}(\text{bpy})_3]^{3+}$. For most of efficient porphyrin sensitizers, introduction of long alkoxy groups to the *ortho*-positions of the two opposite *meso*-phenyls of porphyrin macrocycle provides an efficient “fence” to reduce dye aggregation and impede mass transport of $[\text{Co}(\text{bpy})_3]^{3+/2+}$ to the TiO_2 surface. In **bJS**-series, phenyls with long alkoxy groups are introduced to the opposite β -carbons of porphyrin macrocycle to form a “double fence” structure with expectation of better suppression of molecular aggregation and charge recombination. Therefore, photovoltaic performance of **mJS**- and **bJS**-based DSSCs were fabricated using $[\text{Co}(\text{bpy})_3]^{3+/2+}$ as redox shuttle to understand if double fence porphyrin sensitizers have superior performance to the single fence ones. As shown in Table 2 and Figure 5a, dye loading amount of **mJS**-series are almost two times of **bJS**-series, this difference can be partly ascribed to increased molecular sizes from single to double fences porphyrin sensitizers. Although **bJS** dyes have less uptake than **mJS** dyes, the power conversion efficiency (PCE) of **bJS** dyes are way higher than **mJS** dyes. The PCE of best-performing **bJS**- and **mJS**-based cells were in the ranges of 8.03% to 10.69% and of 2.33% to 6.69%, respectively, clearly demonstrating that double fence porphyrins have superior performance than their single fence counterparts, particularly on the photocurrent.

On the basis of photovoltaic parameters, **bJS**-based cells have both higher J_{SC} and V_{OC} than **mJS** ones, resulting in better PCE, yet no obvious difference in *FF*. In **mJS**-based cells, **mJS1** showed the best PCE of 6.69% with J_{SC} of $10.551 \text{ mA cm}^{-2}$, V_{OC} of 0.833 V, and *FF* of 0.762. Although the BTA- and BTD-incorporated **mJS2** and **mJS3** have more red-shifted absorption spectra than **mJS1**, they exhibited poor J_{SC} of 5.468 and 3.792 mA cm^{-2} , respectively; thus leading to low PCE. Because all three **mJS** dyes have similar extinction coefficient in absorption spectra, the decreased J_{SC} of **mJS2** and **mJS3** is attributed to aggregation of dye molecules. Introduction of anthracene and BTD (or BTA) unit in porphyrin sensitizer extends π -conjugation system but enhances intermolecular π - π interaction at the same time so that aggregation of porphyrin molecules becomes worse. As for **bJS** dyes, they exhibited a trend similar to **mJS** dyes in the absorption

RESEARCH ARTICLE

Table 2. Photovoltaic Parameters of Devices Based on **mJS** dyes, **bJS** dyes, and **YD2-o-C8** under AM1.5G illumination.^[a]

dye	J_{sc} (mA cm ⁻²)	V_{oc} (V)	FF	PCE (%)	Dye loading ^[b] (10 ⁻⁸ mol cm ⁻²)
mJS1	10.551 (9.881 ± 0.595)	0.833 (0.836 ± 0.004)	0.762 (0.767 ± 0.005)	6.69 (6.33 ± 0.33)	7.59 ± 0.22
mJS2	5.468 (5.252 ± 0.224)	0.845 (0.843 ± 0.002)	0.752 (0.754 ± 0.002)	3.48 (3.34 ± 0.14)	7.22 ± 0.63
mJS3	3.729 (3.597 ± 0.128)	0.814 (0.811 ± 0.003)	0.768 (0.769 ± 0.001)	2.33 (2.24 ± 0.08)	7.74 ± 0.99
bJS1	12.525 (12.351 ± 0.158)	0.823 (0.813 ± 0.013)	0.779 (0.785 ± 0.006)	8.03 (7.89 ± 0.16)	4.81 ± 0.52
bJS2	16.586 (16.362 ± 0.376)	0.849 (0.851 ± 0.010)	0.759 (0.759 ± 0.006)	10.69 (10.56 ± 0.12)	4.93 ± 0.14
bJS3	16.483 (16.603 ± 0.119)	0.836 (0.821 ± 0.014)	0.755 (0.754 ± 0.008)	10.42 (10.28 ± 0.22)	4.70 ± 0.31
YD2-o-C8	15.130 (14.665 ± 0.312)	0.849 (0.858 ± 0.008)	0.765 (0.750 ± 0.011)	9.83 (9.44 ± 0.27)	-

[a] Photovoltaic parameters were obtained from the champion cells. Average values of four independent cells with standard error are presented in parentheses.

[b] Obtained by averaging of four independent cells.

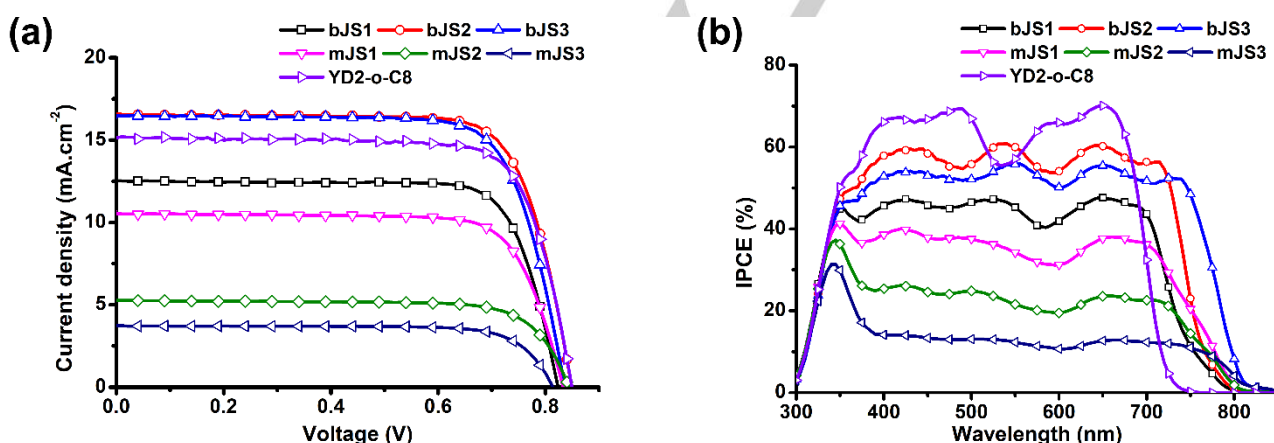


Figure 5. (a) Photocurrent-voltage (J - V) curves under 1 sun illumination and (b) IPCE spectra of **mJS**-series, **bJS**-series, and **YD2-o-C8**.

spectra, therefore their better photovoltaic performance can be attributed to the presence of second fence that helps alleviate dye aggregation and reduce charge recombination. Thus, **bJS2** and **bJS3** exhibit high J_{sc} of 16.586 and 16.483 mA cm⁻¹, respectively, increased by ~60% with respect to the most efficient single fence dye **mJS1**. It should be noted that V_{oc} of **bJS** based cells (0.823 – 0.849 V) are slightly greater than **mJS** based cells (0.814 – 0.845 V). Considering that dye-loading on TiO₂ for **bJS** dyes is much lower than that for **mJS** counterparts, the effects of “double fence” to mitigate charge recombination is pronounced. Importantly, BTA-incorporated **bJS2** and **mJS2** have the highest V_{oc} values of 0.849 and 0.845, respectively, which may be due to further decrease in charge recombination by the presence of a long alkyl chain in BTA moiety. As a result, double fence porphyrin **bJS2** carrying long alkyl chain in acceptor moiety possesses the best photovoltaic performance among all investigated dyes, leading to an impressive PCE of 10.69%, which outperforms the

benchmark **YD2-o-C8** dye (PCE = 9.83% in this work) by 8.7% under same fabrication condition.

The photovoltaic properties of **mJS** and **bJS** dyes are also investigated by incident photon-to-current conversion efficiency (IPCE) spectra in this study. As shown in Figure 5b, **mJS** and **bJS** dyes possess broad IPCE in the visible light region with a smaller dip at around 600 nm when compared to that of **YD2-o-C8** and the onset wavelengths were observed at around 800 nm, which was red-shifted by ca. 60 nm compared to **YD2-o-C8**. The broadened characteristic in IPCE spectra with minor dip between Soret and Q bands echoes the electronic absorption spectra for these new dyes. The plateau heights of IPCE values are in the order of **bJS2** > **bJS3** > **bJS1** > **mJS1** > **mJS2** > **mJS3**, which agree with the trend of J_{sc} values in Table 2. **bJS2** and **bJS3** show much larger coverage and higher plateau than **bJS1**, echoing the importance of BTD and BTA units for enhancing light-harvesting in double fence porphyrin sensitizers as discussed

RESEARCH ARTICLE

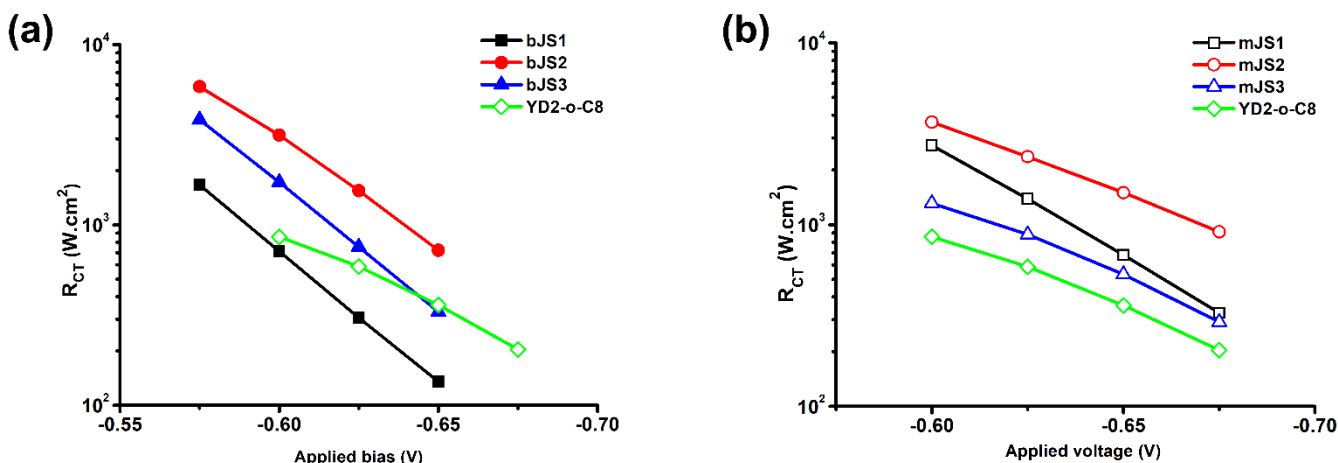


Figure 6. Logarithmic dependence of charge recombination resistance of (a) **bJS** and (b) **mJS** dyes at different applied bias in the dark

above. In contrast, **mJS1** have the best light harvesting efficiency among single fence **mJS**-series, implying that the use of a bigger aromatic bridge would induces more aggregation. Thanks to the double fences at the β -positions in **bJS** series, the presence of BTA and BTD bridges does not cause serious molecular aggregation so that **bJS2** and **bJS3** exhibit excellent cell performance.

To further investigate charge transport and recombination dynamics in the investigated devices, EIS were conducted by applying different bias in the dark. Transmission line model (TLM) was used to extract impedance elements from the spectra. In the medium applied bias region, a 45 degree transmission line appears at high frequency region in Nyquist plot, which represents the charge transport resistance (R_T) in mesoporous TiO_2 film; followed by an arc in the middle frequency, which reflects the charge recombination resistance (R_{CT}) at $\text{TiO}_2/\text{dye}/\text{electrolyte}$ interface (Figure S35a).^[22] Charge transfer resistance at Pt/electrolyte interface (R_P) and diffusion resistance (Z_D) in the electrolyte are too small to be observable. **bJS** dyes exhibit comparable R_{CT} to **mJS** dyes even though dye loading amounts of **bJS** are only half of **mJS** dyes, showing superior ability of **bJS** dyes in suppressing charge recombination. For better comparison, R_{CT} of **bJS** and **mJS** are separately demonstrated in Figure 6 because J_{SC} of two series dyes are significantly different. The order of R_{CT} of **bJS**-series devices is **bJS2** > **bJS3** > **YD2-o-C8** > **bJS1** (Figure 6a), while the order of R_{CT} of **mJS**-series devices is **mJS2** > **mJS1** > **mJS3** > **YD2-o-C8** (Figure 6b). Among double fence **bJS** dyes, **bJS1** exhibits lowest R_{CT} when compares with **bJS2** and **bJS3**, indicating benzoic acid acceptor cannot withdraw electrons efficiently from electron-rich anthracene moiety. Thus, additional strong electron withdrawing groups such as BTA in **bJS2** and BTD in **bJS3** are equipped to enhance charge injection and thus R_{CT} improves. R_{CT} of **bJS2** is higher than that of **bJS3** due to: (1) extra nitrogen atoms of BTA lift the conduction band of TiO_2 , reducing electron recombination, and (2) long alkyl group on nitrogen atom reduces dye aggregation.^[4c] Interestingly, the R_{CT} of double fence **bJS1** is even lower than the one of single fence **YD2-o-C8**, this finding suggests the electron-rich anthracene moiety hampers charge injection to conduction band of TiO_2 , accelerating electron recombination. Thomas et al. reported similar finding that without strong withdrawing group, electron tends to accumulate on

anthracene moiety.^[23] Moreover, 1,2-H atoms of anthracene induce steric congestion between anthracene moiety and nearby aromatic rings, which may also lower intramolecular charge transfer rate.^[24] Similarly, the addition of BTA group increases R_{CT} of **mJS2** compared to **mJS1**. Introduction of BTD in **mJS3**, however, lowers its R_{CT} to even below **mJS1**. R_{CT} of **YD2-o-C8** is the lowest in Figure 6b, which can be explained by its significantly higher J_{SC} when compared with **mJS** dyes. To evaluate charge transport in TiO_2 film, R_T at different applied bias is plotted in Figure S35b. It can be seen that R_T of **mJS** dyes are higher than those in their analogous **bJS** dyes and **YD2-o-C8**, indicating that charge injection from excited dyes in **mJS** based devices are far from sufficient. Similar results were also observed by Wu *et al.*, in which aggregated dye molecules can form a dense layer on TiO_2 surface, blocking charge transfer between oxidized dye and electrolyte.^[25]

Conclusion

Novel double fence porphyrin sensitizers **bJS1**–**bJS3** along with their single fence analogues **mJS1**–**mJS3** have been designed and synthesized. Introduction of acetylene and aromatic units to the donor- π -acceptor backbone successfully achieve extended π -conjugation for both **bJS** and **mJS** sensitizers, leading to decreased HOMO–LUMO gap and improved light harvesting abilities of the sensitizers. However, employment of more aromatic moieties to the molecules enhances intermolecular π - π interaction of sensitizers, resulting in poor J_{SC} and η value (2.33%–6.69%) for **mJS**-based DSSCs. In contrast, **bJS**-based DSSCs exhibited remarkable improvement in photovoltaic performance ($\eta = 8.03\%$ – 10.69%) of DSSCs under the similar conditions. Photovoltaic parameters and EIS spectra show that the major advantages of double fence structure in **bJS** dyes are suppression of dye aggregation and of charge recombination, leading to dramatically improved J_{SC} . As a result, **bJS2** and **bJS3** exhibit high η values of 10.69% and 10.42%, respectively, which are better than the benchmark dye **YD2-o-C8** ($\eta = 9.83\%$) under the similar conditions. We have demonstrated a novel and effective molecular engineering strategy to improve the cell performance of porphyrin dyes. The double fence porphyrin core provides a useful architecture, in which a number of donor, π -

RESEARCH ARTICLE

bridge, and acceptor can be easily introduced to the molecules for use in high-performance DSSCs.

Acknowledgements

This work was supported by the Ministry of Science and Technology, Taiwan (MOST107-2113-M-005-010-MY3 and MOST108-2221-E-007-102-MY3). We thank the Instrument Center at National Chung Hsing University for providing valuable assistance on ESI-MS and FT-IR measurements. We thank to National Center for High-performance Computing (NCHC) for providing computational and storage resources. C.-Y.Y. is also grateful for financial support from the "Innovation and Development Center of Sustainable Agriculture" of The Featured Areas Research Center Program within the framework of the Higher Education Sprout Project by the Ministry of Education (MOE) in Taiwan.

Conflict of interest

The authors declare no conflict of interest.

Keywords: electrochemistry, energy conversion, porphyrinoids, renewable resources

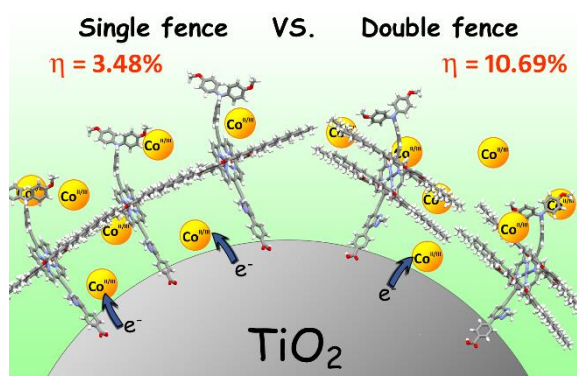
- [1] C. Battaglia, A. Cuevas, S. De Wolf, *Energ. Environ. Sci.* **2016**, *9*, 1552-1576.
- [2] T. L. Jester, *Prog. Photovoltaics* **2002**, *10*, 99-106.
- [3] B. Oregan, M. Gratzel, *Nature* **1991**, *353*, 737-740.
- [4] a) M. Gratzel, *Accounts Chem. Res.* **2009**, *42*, 1788-1798; b) A. Hagfeldt, G. Boschloo, L. C. Sun, L. Kloo, H. Pettersson, *Chem. Rev.* **2010**, *110*, 6595-6663; c) Y. S. Tingare, N. S. Vinh, H. H. Chou, Y. C. Liu, Y. S. Long, T. C. Wu, T. C. Wei, C. Y. Yeh, *Adv. Energy Mater.* **2017**, *7*, 1700032.
- [5] a) M. S. Ahmad, A. K. Pandey, N. Abd Rahima, *Renew. Sust. Energ. Rev.* **2017**, *77*, 89-108; b) Y. J. Son, J. S. Kang, J. Yoon, J. Kim, J. Jeong, J. Kang, M. J. Lee, H. S. Park, Y. E. Sung, *J. Phys. Chem. C* **2018**, *122*, 7051-7060; c) K. Zhu, N. R. Neale, A. Miedaner, A. J. Frank, *Nano Lett.* **2007**, *7*, 69-74; d) S. Mathew, A. Yella, P. Gao, R. Humphry-Baker, B. F. E. Curchod, N. Ashari-Astani, I. Tavernelli, U. Rothlisberger, M. K. Nazeeruddin, M. Gratzel, *Nat. Chem.* **2014**, *6*, 242-247; e) A. Yella, C. L. Mai, S. M. Zakeeruddin, S. N. Chang, C. H. Hsieh, C. Y. Yeh, M. Gratzel, *Angew. Chem. Int. Edit.* **2014**, *53*, 2973-2977; f) Y. Saygili, M. Soderberg, N. Pellet, F. Giordano, Y. M. Cao, A. B. Munoz-Garcia, S. M. Zakeeruddin, N. Vlachopoulos, M. Pavone, G. Boschloo, L. Kavan, J. E. Moser, M. Gratzel, A. Hagfeldt, M. Freitag, *J. Am. Chem. Soc.* **2016**, *138*, 15087-15096; g) Y. J. Wang, T. W. Hamann, *Chem. Commun.* **2018**, *54*, 12361-12364; h) T. Higashino, H. Iiyama, S. Nimura, Y. Kurumisawa, H. Imahori, *Inorg. Chem.* **2020**, *59*, 452-459; i) K. Kannankutty, C.-C. Chen, V. S. Nguyen, Y.-C. Lin, H.-H. Chou, C.-Y. Yeh, T.-C. Wei, *ACS Appl. Mater. Interfaces* **2020**, *12*, 5812-5819; j) A. Yella, H. W. Lee, H. N. Tsao, C. Y. Yi, A. K. Chandiran, M. K. Nazeeruddin, E. W. G. Diau, C. Y. Yeh, S. M. Zakeeruddin, M. Gratzel, *Science* **2011**, *334*, 629-634.
- [6] a) A. Carella, F. Borbone, R. Centore, *Front. Chem.* **2018**, *6*, 481; b) H. A. Maddah, V. Berry, S. K. Behura, *Renew. Sust. Energ. Rev.* **2020**, *121*, 109678.
- [7] a) S. H. Kang, M. J. Jeong, Y. K. Eom, I. T. Choi, S. M. Kwon, Y. Yoo, J. Kim, J. Kwon, J. H. Park, H. K. Kim, *Adv. Energy Mater.* **2017**, *7*, 1602117; b) J.-M. Ji, H. Zhou, H. K. Kim, *J. Mater. Chem. A* **2018**, *6*, 14518-14545.
- [8] M. Gouterman, *J. Mol. Spectrosc.* **1961**, *6*, 138-163.
- [9] a) L. Schmidt-Mende, W. M. Campbell, Q. Wang, K. W. Jolley, D. L. Officer, M. K. Nazeeruddin, M. Gratzel, *Chemphyschem* **2005**, *6*, 1253-1258; b) Q. Wang, W. M. Campbell, E. E. Bonfantani, K. W. Jolley, D. L. Officer, P. J. Walsh, K. Gordon, R. Humphry-Baker, M. K. Nazeeruddin, M. Gratzel, *J. Phys. Chem. B* **2005**, *109*, 15397-15409; c) W. M. Campbell, K. W. Jolley, P. Wagner, K. Wagner, P. J. Walsh, K. C. Gordon, L. Schmidt-Mende, M. K. Nazeeruddin, Q. Wang, M. Gratzel, D. L. Officer, *J. Phys. Chem. C* **2007**, *111*, 11760-11762; d) S. L. Wu, H. P. Lu, H. T. Yu, S. H. Chuang, C. L. Chiu, C. W. Lee, E. W. G. Diau, C. Y. Yeh, *Energ. Environ. Sci.* **2010**, *3*, 949-955.
- [10] a) T. Bessho, S. M. Zakeeruddin, C. Y. Yeh, E. W. G. Diau, M. Gratzel, *Angew. Chem. Int. Edit.* **2010**, *49*, 6646-6649; b) M. K. Nazeeruddin, A. Kay, I. Rodicio, R. Humphrybaker, E. Muller, P. Liska, N. Vlachopoulos, M. Gratzel, *J. Am. Chem. Soc.* **1993**, *115*, 6382-6390; c) C. J. Barbe, F. Arendse, P. Comte, M. Jirousek, F. Lenzmann, V. Shklover, M. Gratzel, *J. Am. Ceram. Soc.* **1997**, *80*, 3157-3171; d) M. K. Nazeeruddin, F. De Angelis, S. Fantacci, A. Selloni, G. Viscardi, P. Liska, S. Ito, T. Bessho, M. Gratzel, *J. Am. Chem. Soc.* **2005**, *127*, 16835-16847; e) Q. J. Yu, Y. H. Wang, Z. H. Yi, N. N. Zu, J. Zhang, M. Zhang, P. Wang, *ACS Nano* **2010**, *4*, 6032-6038.
- [11] a) S. Chang, H. Wang, L. T. Lin Lee, S. Zheng, Q. Li, K. Y. Wong, W.-K. Wong, X. Zhu, W.-Y. Wong, X. Xiao, T. Chen, *J. Mater. Chem. C* **2014**, *2*, 3521-3526; b) J.-W. Shiu, Y.-C. Chang, C.-Y. Chan, H.-P. Wu, H.-Y. Hsu, C.-L. Wang, C.-Y. Lin, E. W.-G. Diau, *J. Mater. Chem. A* **2015**, *3*, 1417-1420; c) K. Zeng, Y. Chen, W.-H. Zhu, H. Tian, Y. Xie, *J. Am. Chem. Soc.* **2020**, *142*, 5154-5161; d) J. M. Ji, H. R. Zhou, Y. K. Eom, C. H. Kim, H. K. Kim, *Adv. Energy Mater.* **2020**, *10*, 2000124.
- [12] a) C.-Y. Lin, Y.-C. Wang, S.-J. Hsu, C.-F. Lo, E. W.-G. Diau, *J. Phys. Chem. C* **2010**, *114*, 687-693; b) M. Tanaka, S. Hayashi, S. Eu, T. Umeyama, Y. Matano, H. Imahori, *Chem. Commun.* **2007**, 2069-2071; c) C. L. Mai, W. K. Huang, H. P. Lu, C. W. Lee, C. L. Chiu, Y. R. Liang, E. W. G. Diau, C. Y. Yeh, *Chem. Commun.* **2010**, *46*, 809-811; d) Y. Kurumisawa, T. Higashino, S. Nimura, Y. Tsuji, H. Iiyama, H. Imahori, *J. Am. Chem. Soc.* **2019**, *141*, 9910-9919; e) T. Higashino, Y. Kurumisawa, S. Nimura, H. Iiyama, H. Imahori, *Eur. J. Org. Chem.* **2018**, *2018*, 2537-2547.
- [13] a) T. Higashino, Y. Fujimori, K. Sugiura, Y. Tsuji, S. Ito, H. Imahori, *Angew. Chem. Int. Edit.* **2015**, *54*, 9052-9056; b) T. Higashino, Y. Kurumisawa, N. Cai, Y. Fujimori, Y. Tsuji, S. Nimura, D. M. Packwood, J. Park, H. Imahori, *ChemSuschem* **2017**, *10*, 3347-3351; c) T. Higashino, S. Nimura, K. Sugiura, Y. Kurumisawa, Y. Tsuji, H. Imahori, *ACS Omega* **2017**, *2*, 6958-6967.
- [14] a) S. H. Kang, S. Y. Jung, Y. W. Kim, Y. K. Eom, H. K. Kim, *Dyes Pigments* **2018**, *149*, 341-347; b) H. Zhou, J.-M. Ji, S. H. Kang, M. S. Kim, H. S. Lee, C. H. Kim, H. K. Kim, *J. Mater. Chem. C* **2019**, *7*, 2843-2852; c) J.-M. Ji, S. H. Kim, H. Zhou, H. K. Kim, H. K. Kim, *ACS Appl. Mater. Interfaces* **2019**, *11*, 24067-24077.
- [15] a) C. W. Lee, H. P. Lu, C. M. Lan, Y. L. Huang, Y. R. Liang, W. N. Yen, Y. C. Liu, Y. S. Lin, E. W. G. Diau, C. Y. Yeh, *Chem.-Eur. J.* **2009**, *15*, 1403-1412; b) G. Yang, Y. Tang, X. Li, H. Ågren, Y. Xie, *ACS Appl. Mater. Interfaces* **2017**, *9*, 36875-36885; c) S. Mathew, N. A. Astani, B. F. E. Curchod, J. H. Delcamp, M. Marszalek, J. Frey, U. Rothlisberger, M. K. Nazeeruddin, M. Grätzel, *J. Mater. Chem. A* **2016**, *4*, 2332-2339; d) K. Zeng, Z. Tong, L. Ma, W.-H. Zhu, W. Wu, Y. Xie, *Energ. Environ. Sci.* **2020**, Advance Article.
- [16] Y. Lu, H. Song, X. Li, H. Ågren, Q. Liu, J. Zhang, X. Zhang, Y. Xie, *ACS Appl. Mater. Interfaces* **2019**, *11*, 5046-5054.
- [17] a) C. L. Wang, M. Zhang, Y. H. Hsiao, C. K. Tseng, C. L. Liu, M. F. Xu, P. Wang, C. Y. Lin, *Energ. Environ. Sci.* **2016**, *9*, 200-206; b) J. Pan, H. Song, C. Lian, H. Liu, Y. Xie, *Dyes Pigments* **2017**, *140*, 36-46; c) J. V. S. Krishna, D. Koteswar, T. H. Chowdhury, S. P. Singh, I. Bedja, A. Islam, L. Giribabu, *J. Mater. Chem. C* **2019**, *7*, 13594-13605.
- [18] a) C. Y. Lee, J. T. Hupp, *Langmuir* **2010**, *26*, 3760-3765; b) H.-H. Chou, K. S. K. Reddy, H.-P. Wu, B.-C. Guo, H.-W. Lee, E. W.-G. Diau, C.-P. Hsu, C.-Y. Yeh, *ACS Appl. Mater. Interfaces* **2016**, *8*, 3418-3427.
- [19] P. Devasthale, W. Wang, J. Mignone, K. Renduchintala, S. Radhakrishnan, J. Dhanapal, J. Selvaraj, R. Kuppusamy, M. A. Pellemounter, D. Longhi, N. Huang, N. Flynn, A. V. Azzara, K. Rohrbach, J. Devenny, S. Rooney, M. Thomas, S. Glick, H. Godonis, S. Harvey, M.

RESEARCH ARTICLE

- J. Cullen, H. Zhang, C. Caporuscio, P. Stetsko, M. Grubb, C. Huang, L. Zhang, C. Freeden, B. J. Murphy, J. A. Robl, W. N. Washburn, *Bioorg. Med. Chem. Lett.* **2015**, 25, 4412-4418.
- [20] O. Robles, F. E. McDonald, *Org. Lett.* **2008**, 10, 1811-1814.
- [21] T. Nakagawa, J. Hatano, Y. Matsuo, *J. Porphyr. Phthalocya.* **2014**, 18, 735-740.
- [22] a) F. Fabregat-Santiago, J. Bisquert, G. Garcia-Belmonte, G. Boschloo, A. Hagfeldt, *Sol. Energy Mater. Sol. Cels* **2005**, 87, 117-131; b) J. Bisquert, *Phys. Chem. Chem. Phys.* **2000**, 2, 4185-4192.
- [23] K. R. J. Thomas, P. Singh, A. Baheti, Y. C. Hsu, K. C. Ho, J. T. Lin, *Dyes Pigments* **2011**, 91, 33-43.
- [24] a) C. Teng, X. C. Yang, C. Yang, S. F. Li, M. Cheng, A. Hagfeldt, L. C. Sun, *J. Phys. Chem. C* **2010**, 114, 9101-9110; b) R. Y. Y. Lin, H. W. Lin, Y. S. Yen, C. H. Chang, H. H. Chou, P. W. Chen, C. Y. Hsu, Y. C. Chen, J. T. Lin, K. C. Ho, *Energ. Environ. Sci.* **2013**, 6, 2477-2486.
- [25] C. H. Wu, M. C. Chen, P. C. Su, H. H. Kuo, C. L. Wang, C. Y. Lu, C. H. Tsai, C. C. Wu, C. Y. Lin, *J. Mater. Chem. A* **2014**, 2, 991-999.

RESEARCH ARTICLE

Entry for the Table of Contents



Double fence porphyrin dyes **bJS1–bJS3** were designed and synthesized for high efficiency dye-sensitized solar cells (DSSCs). Compared to typical single fence porphyrin dyes, double fence porphyrins show reduced dye aggregation and charge recombination, which are evidenced by photovoltaic data, thus giving much better device performance than their single fence counterparts.